

## MODEL AND ANALYSIS OF THE PROCESS OF UNIT-LOAD STREAM SORTING BY A MANIPULATOR WITH TORSIONAL DISKS

TOMASZ PIĄTKOWSKI

*University of Technology and Life Sciences, Department of Postal Technology, Bydgoszcz, Poland  
e-mail: tomasz.piatkowski@utp.edu.pl*

In the paper, the author presents a proposal for the modelling of the process of sorting of a stream of unit loads realised by means of a manipulator with torsional disks. In the developed model, one takes into account three zones of friction influencing motion of the load in the manipulator working space: the first one associated with interactions on the manipulator active carrying surface, and two zones located on the belt conveyor right in front of, and behind the manipulator. Frictional properties of the object are represented by a nonlinear friction coefficient defined based on a cubic b-spline curve. On the basis of numerical experiments performed on the sorting model, one determined the influence of fundamental structural and operational parameters of the manipulator on precision and reliability of the process of unit-load stream sorting. The obtained data can be used as guidelines for designing new solutions of sorting manipulators and may provide hints necessary for optimization of already-existing devices.

*Key words:* unit load, dry friction, handling process, belt conveyor, sorting

### 1. Introduction

In transportation centres, where concentration of transported goods is high, one needs to automatically handle the stream of unit loads (i.e. objects having the form of cuboidal parcels). For this purpose, one uses highly efficient no-grip type manipulators, i.e. manipulators constructed on the basis of a belt conveyor or a link-belt conveyor, which have no gripping devices, and act on the objects through a push, or through a sequence of pushes or strikes (Akella *et al.*, 2000; Mason, 1999; Piątkowski, 2004).

One of typical manipulation actions is, among other things, the process of sorting. It consists in dividing the stream of loads (according to the criteria recognised by the scanning device in the transport system) into several new transportation ways. However, forcing a new direction of motion requires that a force impulse of adequate magnitude is exerted on the load at the right moment. One of the ways for realising this task is application of devices, whose working elements are active carrying surfaces of the conveyor on which the transported loads lie. A practical implementation of this concept are stream manipulators with trays (built on the basis of link-belt conveyors – Tilt-tray Sorter<sup>1</sup>, Cross Belt Sorter<sup>2</sup> and stationary manipulators (incorporated into the belt conveyor) in the form of a system of driven disks or rolls which allow for controlling (programming) the direction of the friction field that exerts force on the load (ProSort SC1<sup>3</sup>, Autosort 5<sup>4</sup>, ProSort SRT<sup>5</sup>, Single Powered Pivot Diverter<sup>6</sup>).

In the available literature, Böhringer *et al.* (2000), Laowattana and Satachakul (1999), Luntz *et al.* (1997), disk manipulators are considered as devices realising the process of positioning and rotating the objects on conveyors. The research works concerned with this problem deal with the analysis of control systems of microactuators (independently driven disks of two degrees of freedom) equipped with an elaborated system of sensors controlling the current position of load and taking it to a precisely defined destination position. In the subject literature, however, one can not find any description of application of this kind of devices in a highly efficient process of load sorting,

---

<sup>1</sup>Tilt-tray Sorter DDS, accessed 2007-10-27, Commercial folder published by Man-  
nesmann Dematic AG, Offenbach, Germany, [www.dematic.com](http://www.dematic.com)

<sup>2</sup>Cross Belt Sorter, accessed 2008-07-24, Commercial folder published by Wally  
Transport Systems Inc, Longboat Key, FL, USA,  
[www.wallysorter.com/pdfs/ally\\_Cross\\_Belt\\_Sorter\\_Overview.pdf](http://www.wallysorter.com/pdfs/ally_Cross_Belt_Sorter_Overview.pdf)

<sup>3</sup>ProSort SC1, accessed 2008-07-28, Commercial folder published by Hytrol Co-  
nveyor Company Inc., Jonesboro, AR, USA,  
[www.hytrol.com/mediacenter/catalog\\_sheets/ca\\_prosortsc.pdf](http://www.hytrol.com/mediacenter/catalog_sheets/ca_prosortsc.pdf)

<sup>4</sup>Autosort 5 – Pop-Up Wheel Sorter, accessed 2008-07-24, Commercial folder pu-  
blished by Automation Inc., Oak Lawn, IL, USA,  
[www.automotionconveyors.com/media/print\\_media/products/sc5\\_popupwheel.pdf](http://www.automotionconveyors.com/media/print_media/products/sc5_popupwheel.pdf)

<sup>5</sup>ProSort SRT, accessed 2008-12-10, Commercial folder published by Hytrol Co-  
nveyor Company Inc., Jonesboro, AR, USA,  
[www.hytrol.com/mediacenter/catalog\\_sheets/ca\\_prosortsrt.pdf](http://www.hytrol.com/mediacenter/catalog_sheets/ca_prosortsrt.pdf)

<sup>6</sup>Single Powered Pivot Diverter, accessed 2008-12-10, Commercial folder published  
by Hytrol Conveyor Company Inc., Jonesboro, AR, USA,  
[www.mckessockconveyors.com/PDF/Hytrol/overheadpush\\_singleppd.pdf](http://www.mckessockconveyors.com/PDF/Hytrol/overheadpush_singleppd.pdf)

in which the role of sensors is reduced to bi-state detection of the presence of load in the working space of the manipulator.

The general knowledge of application of the sorting manipulators with torsional disks is based only on the data contained in information booklets published by the companies specializing in production and delivery of complete distribution systems (ProSort SC1, Autosort 5, ProSort SRT, Single Powered Pivot Diverter). The contents of these booklets do not allow one to get through to the information characterising the course of the realised process of sorting, neither can one learn about imperfections of the process and their causes. There are no data that would facilitate introduction of adequate changes, e.g. constructional improvements or changes in operational parameter settings, which could remove the imperfections appearing in the course of the sorting process.

In order to objectively assess the basic utility features of the concept of a manipulator with torsional disks, one undertook an attempt of developing a dynamic model of the load stream distribution process. The data obtained from numerical experiments carried out on the proposed model can be used for formulating necessary assumptions and guidelines, applicable when one designs a disk manipulator satisfying concrete exploitation requirements.

## 2. Working conditions of the manipulator

The sorting manipulators with torsional disks are allocated along the belt conveyor and built into its structure (Fig. 1a). The role of executing elements is played by a system of power-driven disks, which constitute the active carrying surface for the transported loads. For the purpose of planned investigations, we assumed that the disks have two degrees of freedom: rolling motion about the horizontal axis  $x_1$ , and rotary motion about the vertical axis  $x_2$  made when a change of the load transport direction is forced (Fig. 1b – according to Luntz *et al.* (1997)). In the neutral position, the disks take the angle of  $\alpha = 0^\circ$ , which makes it possible to send the loads to more distant reception lines. The working position of the disks corresponds to the inclination angle of the reception lines with respect to the main stream. We assume that this angle is held in the range of  $\alpha = 30^\circ$ - $90^\circ$ .

The idea of active carrying surface with power-driven disks rotating about the axes  $x_1$  and  $x_2$ , having a great range of the working angle  $\alpha$  is complicated from the constructional point of view. For the sake of simplification of the disk

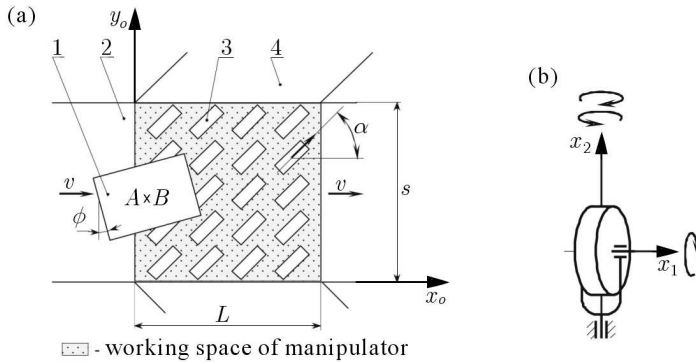


Fig. 1. Illustrative diagram of a manipulator with torsional disks: (a) working space of the manipulator, (b) degrees of freedom of the manipulator executing element (rotational motions about axes  $x_1$  and  $x_2$ ); 1 – unit load, 2 – main conveyor, 3 – executing element of the manipulator (system of power-driven disks), 4 – chute,  $v$  – transportation velocity of the main conveyor,  $\alpha$  – working angle of disk setting,  $s$  – width of the main conveyor

drive, one applies two variants of solutions, depending on the assumed working angle  $\alpha$  of the disks.

In the case of devices which carry away the loads from the main conveyor at an angle of  $\alpha = 30^\circ$ , one uses pairs of coupled torsional disks (Fig. 2a). Each pair is set in rotational motion about the axis  $x_1$  by means of a driving strand of circular cross-section, taking the drive from the main conveyor belt (ProSort SC1) or from an electric motor (Single Powered Pivot Diverter). The torsional motion of individual pairs of disks about the axis  $x_2$  is effected by a lever system connected to a pneumatic cylinder. These devices are adapted for distributing loads to both sides, relative to the main conveyor axis.

When the carry-away angle in the sorting device takes a high value, i.e.  $\alpha = 90^\circ$  (Fig. 2b – ProSort SRT), or  $\alpha = 45^\circ$  (Autosort 5), one usually applies another solution in which all the disks have the same constant working angle ( $\alpha = \text{const}$ ) and are driven by a common drive and make rotational motion about the axis  $x_1$ . The ability of sorting the loads is achieved through action that consists in either preventing the manipulated object and the disk from being in contact or causing that they enter into such a contact. This is achieved by exposing or hiding the disks with respect to the surface of the main conveyor through translational motion in the vertical direction  $x_2$ ; the motion is made by the set of disks or by some segments of the carrying surfaces (the segments placed in the spaces between the disks responsible for the flow of loads to more distant chutes – (3) Fig. 2b). The systems of disks having the working angle

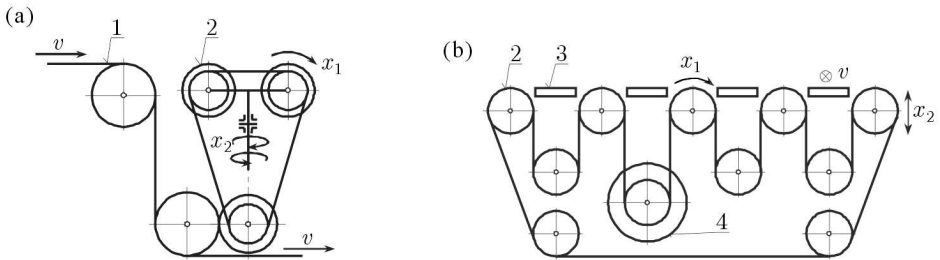


Fig. 2. Example solutions of power drive transfer onto disks of the manipulator with respect to the working angle of disks  $\alpha$ : (a) when  $\alpha = 30^\circ$  – ProSort SC1, Single Powered Pivot Diverter, (b) when  $\alpha = 90^\circ$  – ProSort SRT, or  $\alpha = 45^\circ$  – Autosort 5;  $x_1$  and  $x_2$  – degrees of freedom of the manipulator executing element, 1 – surface of main conveyor, 2 – carrying surface of the disk system, 3 – carrying surfaces responsible for the flow of loads (along main conveyor) to more distant chutes, 4 – electric motor,  $v$  – transportation velocity of the main conveyor

of  $\alpha = 90^\circ$  are adapted to carrying-away the manipulated loads to both sides, while those having the angle of  $\alpha = 45^\circ$  – only to one side.

In the assessment of the course of load manipulation process, two basic criteria have essential meaning: protection of the load from damage and reliability of the operations the manipulator is expected to realise. As far as the first criterion is concerned, one can take the assumption that the manipulated loads should not be endangered to any mechanical damage – the course of interaction forces exerted on the manipulated loads must then have a gentle character (they result only from frictional contact between the carrying surfaces of the object and the manipulator).

To assess the process according to the second criterion, one must acquire data describing the influence of parameters of the sorting process on motion of the manipulated object. These data have been obtained by means of numerical experiments on the mathematical model described in a further part of the paper. One of the most essential components of this model is description of dry friction phenomenon.

### 3. Dry-sliding friction

The coefficient of dry friction depends on the kind of surfaces of bodies engaged in frictional contact, quality (state of roughness) of the surfaces, ambient temperature and humidity, and the rubbing speed. Additionally, for a given

pair of bodies rubbing one against another in specific ambient conditions, the most important factor influencing the friction coefficient value is the speed of rubbing (Hensen, 2002).

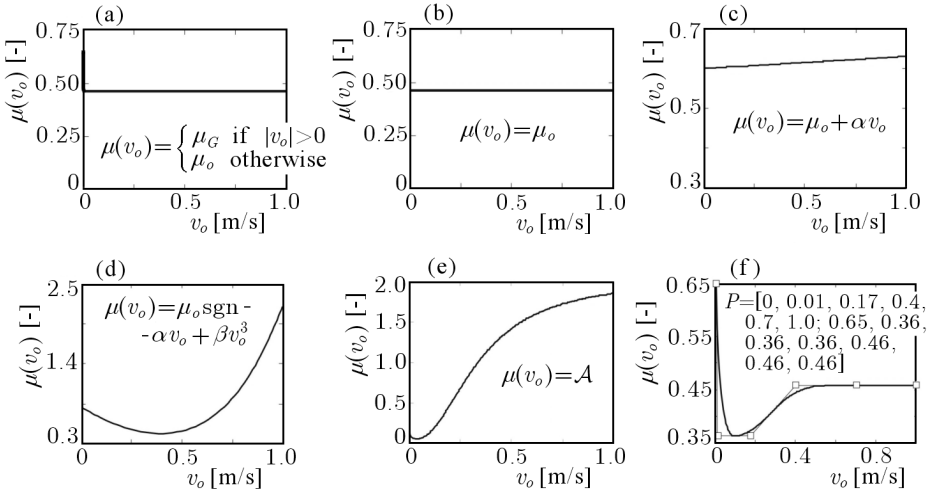


Fig. 3. Exemplary courses of the dry friction coefficient in function of the rubbing speed: (a) constant two-parameter – Tarnowski and Bartkiewicz (1998), (b) constant single-parameter – Tarnowski and Bartkiewicz (1998), (c) linear – Krivoplas (1980), (d) polynomial – Awrejcewicz (1984), (e) two Stribeck curves – Awrejcewicz and Olejnik (2002), (f) b-spline curve – Piątkowski and Sempruch (2006b); parameter values  $(\alpha, \beta, b_1, b_2, b_3, c, \mu_o, \mu_{min}, v_{min})$  are taken from the cited literature where

$$\mathcal{A} = \begin{cases} \mu_{min} + (\mu_o - \mu_{min}) \exp(-b_1|v_o|) & \text{if } |v_o| < v_{min} \\ \left( \begin{array}{l} \mu_{min} + (\mu_o - \mu_{min}) \exp(-b_1|v_o|) + \\ + \frac{b_2 b_3 (|v_o| - v_{min})}{1 + b_2 (|v_o| - v_{min})} \end{array} \right) & \text{if } |v_o| > v_{min} \\ \mu_o & \text{otherwise} \end{cases}$$

In contemporary literature, one can find many diverse characteristics of the friction coefficient proposed for description of dry friction. Exemplary courses of these characteristics (drawn in function of the rubbing speed  $v_o = 0-1$  m/s – the interval pertaining to a sorting process of moderate intensity, Piątkowski and Sempruch (2006a,b, 2008a,b)) are presented in Fig. 3. In most cases, they have an idealised linear character (Krivoplas, 1980; Tarnowski and Bartkiewicz, 1998 – Fig. 3a-c), or sometimes a nonlinear course, and are usually valid in a narrow range of the rubbing speed (Awrejcewicz, 1984; Awrejcewicz and

Olejnik, 2002 – Fig. 3d,e). The applicability of the presented descriptions of friction (to the considered application) can be preliminarily assessed on the basis of analysis of friction coefficient variability shown in graphs. The graphs in Fig. 3a-c present a logical and real range of variability of the friction coefficient. On the other hand, the courses of characteristics in Fig. 3d,e show that the applicability of these characteristics is limited to cases when only low rubbing speeds may appear – for the speed approaching  $v_o = 1$  m/s, the friction coefficient would reach an unbelievably high value.

The characteristic of friction coefficient should be valid in a wide range of the rubbing speed. The transport of the load stream via lines of automated sorting may result in rubbing of the objects against working surfaces of the manipulator with the speed exceeding  $v_o = 0-2.5$  m/s (Piątkowski and Sempruch, 2008a,b). The results of experimental investigations on friction in this range of velocity and a proposal for a new characteristic of the friction coefficient (for an object made of cardboard sliding on a belt made of rubber, Fig. 3f) are presented by Piątkowski and Sempruch (2006b). The characteristic is defined by a cubic b-spline curve with six control points.

From among the hereinafter presented characteristics of the friction coefficient, we select the characteristic of Fig. 3f as the one which most faithfully represents the physical nature of friction in the process of manipulation of unit loads. The analysis of results of model simulation of the sorting process, taking into account different ways of description of the friction coefficient, is presented in a further part of this study (in Section 6).

Particular difficulties in determining the friction force one can encounter in the range of rubbing speeds close to zero, where the phenomenon of stick-slip appears (Tarnowski and Bartkiewicz, 1998). This phenomenon is accompanied by a rapid change of frictional resistance, and it has an important meaning i.e. in robotics, when one deals with precise positioning of robot's members (Korendo and Uhl, 1998).

For the needs of the present study, we used the following expression to describe analytical relationships taking into account nonlinearity of the friction force resulting from static and kinetic friction

$$F = \begin{cases} F_{kin} \operatorname{sgn}(v_o) & \text{if } |v_o| > v_{min} \\ \left\{ \begin{array}{ll} P_{ext} & \text{if } F_{stat} > |P_{ext}| \\ F_{stat} \operatorname{sgn}(P_{ext}) & \text{otherwise} \end{array} \right\} & \text{otherwise} \end{cases} \quad (3.1)$$

where

- $P_{ext}$  – external force exerted on the object, tangent to resistance surface
- $F_{kin}$  – kinetic friction force
- $F_{stat}$  – limiting static friction force.

The quantity  $v_{min}$  (in expression (3.1)) makes up the threshold speed of a small magnitude (assumed in the paper,  $v_{min} = 10^{-6}$  m/s), below which the rubbing speed is considered zero (Kikuuwe *et al.*, 2005). The use of the threshold speed allows one to overcome difficulties which occur during numeric integration of equations of motion containing a non-continuous friction model (when  $v_o = 0$ ).

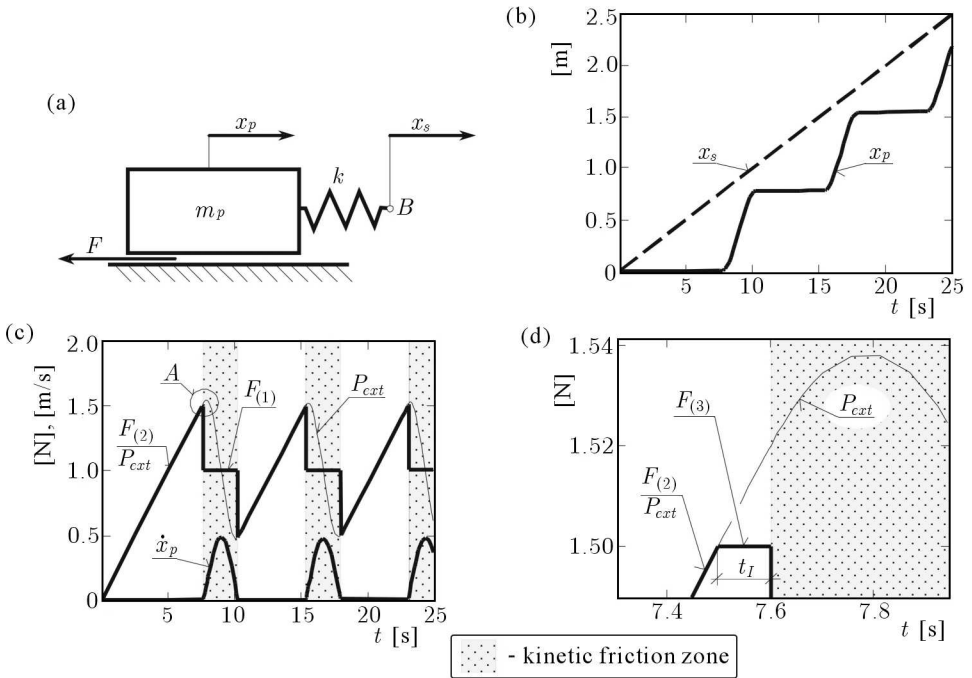


Fig. 4. Results of dry friction simulation: (a) diagram of the mechanical system, (b) trajectory motion of the object and spring end  $B$ , (c) course of the friction force, external force and rubbing speed, (d) detail  $A$  of Fig. 4c in magnification;  $m_p = 1$  kg,  $F_{kin} = 1$  N,  $F_{stat} = 1.5$  N,  $k = 2$  N/m,  $\dot{x}_s = 0.1$  m/s,  $v_{min} = 0.001$  m/s,  $P_{ext} = k(x_s - x_p)$ ,  $t_I$  – duration of stage  $F_{(3)}$  in the first cycle of stick-slip friction

Activity of respective rows of formula (3.1) is illustrated in Fig. 4b,c,d. The graphs are assigned on the basis of simulation of the object motion in stick-slip friction conditions (Fig. 4a). The following data was accepted during the simulation:  $m_p = 1$  kg,  $F_{kin} = 1$  N,  $F_{stat} = 1.5$  N,  $k = 2$  N/m,  $\dot{x}_s = 0.1$  m/s,

$v_{min} = 0.001$  m/s, initial conditions –  $x_p(t=0) = 0$ ,  $\dot{x}_p(t=0) = 0$ ,  $x_s(t=0) = 0$ . Symbols  $F_{(1)}$ ,  $F_{(2)}$  and  $F_{(3)}$  presented in Fig. 4 relate to the successive rows of equation (3.1). The first row  $F_{(1)}$  represents kinetic friction, the second  $F_{(2)}$  and third  $F_{(3)}$  – static friction. The row marked as  $F_{(2)}$  is responsible for the body maintenance at rest (when the external force  $P_{ext}$  is smaller than the static friction force  $F_{stat}$ ), and row  $F_{(3)}$  – for the initiation of the body transition from the state of static friction to kinetic friction (when the external force  $P_{ext}$  becomes larger than the static friction force  $F_{stat}$ ).

The value of threshold speed is chosen on the basis of experience and the explorer's intuition. In Fig. 5, the influence of the threshold speed  $v_{min}$  on duration of friction static stage  $F_{(3)}$  is shown. A strict relationship between the speed threshold value  $v_{min}$  and duration of stage  $F_{(3)}$  occurs during the first body transition from the state of static friction to the kinetic one (curve marked by  $t_I$ ). The next cycles of the stick-slip friction (curves  $t_{II}$  and  $t_{III}$ ) do not show such a dependence. The obtained effect is caused by the fact that the first stick-slip cycle occurs when the initial speed of the object  $\dot{x}_p = 0$ , and the next – when  $|\dot{x}_p| \leq v_{min}$ .

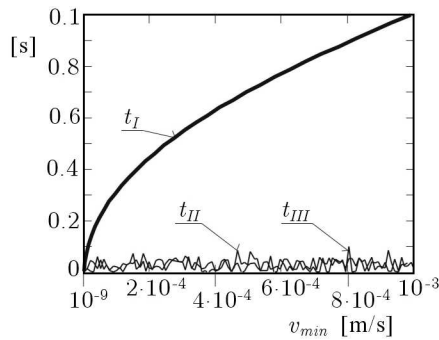


Fig. 5. Graph of duration of static friction stage  $F_{(3)}$  in function of the threshold velocity  $v_{min}$  (when  $F_{stat} \leq |P_{ext}|$ , according to equation (3.1));  $t_I$ ,  $t_{II}$ ,  $t_{III}$  – duration of static friction stage  $F_{(3)}$  of successive stick-slip cycles

#### 4. Model of load motion

The motion of a load in the working space of the manipulator is evoked by the carrying surfaces which can be divided into three zones (Fig. 6):  $b$  – that includes the manipulator-load interaction area, and  $a$  and  $c$  that are located on the main conveyor just in front of the manipulator and behind it.

Depending on dimensions and position of the load and width of the zone  $b$ , the load can be in contact with one, two or with all zones simultaneously.

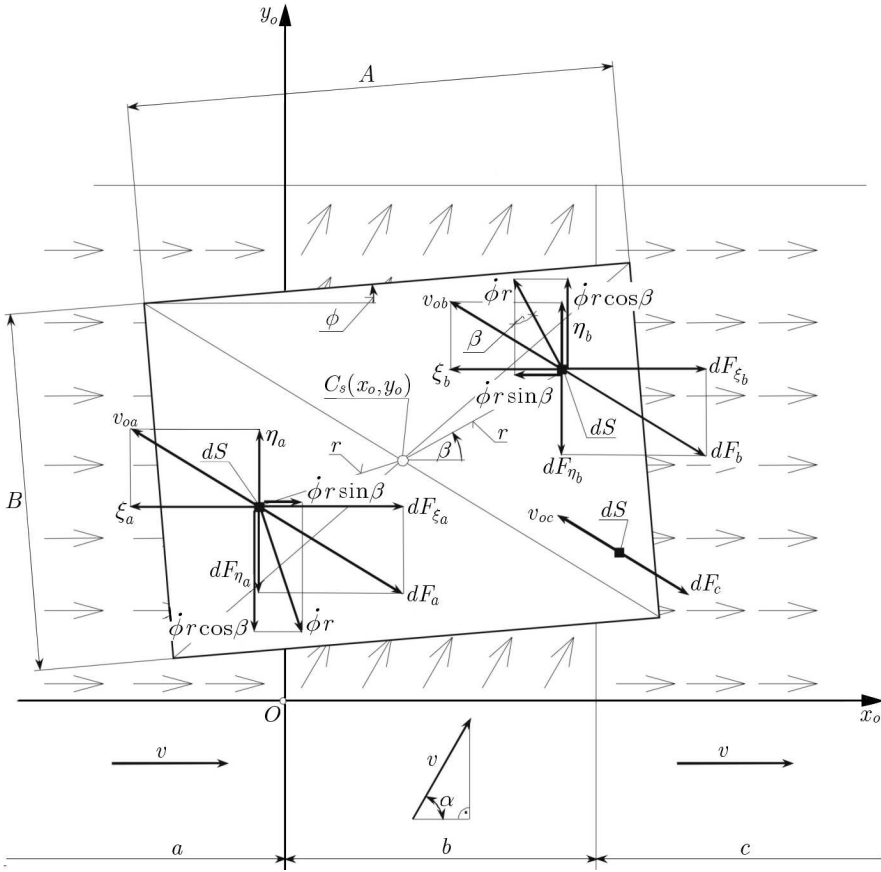


Fig. 6. Scheme of forces acting on the object during sorting by the manipulator with torsional disks;  $A \times B$  – load dimensions,  $\phi$  – angle of load rotation with respect to gravity center  $C_s$ ,  $dS$  – infinitesimal surface,  $v_{oa}$ ,  $v_{ob}$ ,  $v_{oc}$  – resulting rubbing speed of the infinitesimal friction surface  $dS$  in zones  $a$ ,  $b$  and  $c$ ,  $\xi_a$ ,  $\xi_b$ ,  $\xi_c$ ,  $\eta_a$ ,  $\eta_b$ ,  $\eta_c$  – components of the rubbing speed,  $dF_a$ ,  $dF_b$ ,  $dF_c$  – infinitesimal friction force in the zones  $a$ ,  $b$  and  $c$  (friction force has the direction of the rubbing speed and has an opposite sense in relation to it),  $dF_{\xi a}$ ,  $dF_{\xi b}$ ,  $dF_{\xi c}$ ,  $dF_{\eta a}$ ,  $dF_{\eta b}$ ,  $dF_{\eta c}$  – components of the friction force,  $v$  – conveyor velocity of transportation

In the physical model of load sorting, one assumes a rectangular reference coordinate system  $Ox_o y_o$  connected with the manipulator frame, whose origin coincides with the border of the zone  $b$ , and the direction of the axis  $x_o$  is consistent with the axis of the main conveyor (Fig. 6). Additionally:

- the friction zones  $a$ ,  $b$  and  $c$  of the conveyor lie in one plane,
- the power-driven disks of the manipulator are free of axis-direction error, i.e. they do not exhibit any lateral whip,
- the disks and dead zones located between them have dimensions much smaller than those of the manipulated objects,
- the load is treated as a rigid body with uniformly distributed mass,
- the influence of random disturbances is neglected,
- the friction phenomenon is described according to Coulomb's model (and its modifications, Kikuuwe *et al.* (2005)),
- one takes into account the existence of static and kinetic friction which can appear in the following configurations:
  - lack of static friction in all zones simultaneously,
  - kinetic friction in the zones  $a$  and  $c$ , and static friction in the zone  $b$ ,
  - kinetic friction in the zone  $b$ , and static friction in the zones  $a$  and  $c$ ,
- one assumes identical frictional properties in the zones  $a$  and  $c$ , and the same conveyor transportation speed  $v$  in these zones.

The planar motion of the load on the conveyor and the manipulator disk surfaces is described in the rectangular system of coordinates  $Ox_o y_o$  by the following system of equations (according to Fig. 6)

$$\begin{aligned}
 m_p \ddot{x}_o &= F_{\xi ac} + F_{\xi b} & m_p \ddot{y}_o &= -F_{\eta ac} - F_{\eta b} \\
 I_p \ddot{\phi} &= -T_{ac} - T_b
 \end{aligned}
 \tag{4.1}$$

where:  $F_{(j)ac}$ ,  $F_{(j)b}$  are components of the load friction force in the zones  $a$ ,  $c$  and  $b$ ,  $j = \xi, \eta$

$$F_{(j)ac} = \left\{ \begin{array}{ll} F_{ac\ max} \frac{j_{ac}}{v_{oac}} & \text{if } v_{oac} > v_{min} \\ \left\{ \begin{array}{ll} -F_{b\ max} \frac{j_b}{v_{ob}} & \text{if } F_{ac\ max} > F_{b\ max} \\ -F_{ac\ max} \frac{j_b}{v_{ob}} & \text{otherwise} \end{array} \right\} & \text{otherwise} \end{array} \right.$$

$$F_{(j)b} = \begin{cases} F_{bmax} \frac{j_b}{v_{ob}} & \text{if } v_{ob} > v_{min} \\ \left\{ \begin{array}{ll} -F_{acmax} \frac{j_{ac}}{v_{oac}} & \text{if } F_{bmax} > F_{acmax} \\ -F_{bmax} \frac{j_{ac}}{v_{oac}} & \text{otherwise} \end{array} \right\} & \text{otherwise} \end{cases} \quad (4.2)$$

$$F_{acmax} = F_{amax} + F_{cmax}$$

$F_{(i)max}$  is the limit friction force acting between the load and carrying surface of the manipulator in the zones  $i = a, b, c$

$$F_{(i)max} = \frac{m_p g}{S} \int_{S_i} \mu_i w_i dS \quad (4.3)$$

$T_{ac}, T_b$  – moments of load friction forces in the friction zones  $a, c$  and  $b$

$$T_{ac} = \begin{cases} T_{acmax} & \text{if } |\dot{\phi}| > \phi_{min} \\ \left\{ \begin{array}{ll} -T_{bmax} & \text{if } T_{acmax} > |T_{bmax}| \\ -T_{acmax} \operatorname{sgn}(T_{bmax}) & \text{otherwise} \end{array} \right\} & \text{otherwise} \end{cases}$$

$$T_b = \begin{cases} T_{bmax} & \text{if } |\dot{\phi}| > \phi_{min} \\ \left\{ \begin{array}{ll} -T_{acmax} & \text{if } T_{bmax} > |T_{acmax}| \\ -T_{bmax} \operatorname{sgn}(T_{acmax}) & \text{otherwise} \end{array} \right\} & \text{otherwise} \end{cases} \quad (4.4)$$

$$T_{acmax} = T_{amax} + T_{cmax}$$

$T_{(i)max}$  – moment of the limit friction force of the load in the zones  $i = a, b, c$

$$T_{(i)max} = \begin{cases} \frac{m_p g}{S} \int_{S_i} \mu_i \frac{w_i}{v_{oi}} [\eta_i(x_s - x_o) + \xi_i(y_s - y_o)] dS & \text{if } v_{io} > v_{min} \\ \frac{m_p g}{S} \mu_i \int_{S_i} w_i r dS & \text{otherwise} \end{cases} \quad (4.5)$$

$w_i$  – function describing geometry of the load surface;  $w_i = 1$  in cases when the load is in contact with the conveyor in the zone  $i$ , otherwise –  $w_i = 0$

$S = AB$  – carrying surface of the load

$r$  – distance between the infinitesimal surface  $dS$  and gravity centre of the load  $C_s$

$$r = \sqrt{(x_s - x_o)^2 + (y_s - y_o)^2} \quad (4.6)$$

$dS$  – infinitesimal surface

$\xi_a, \xi_b, \xi_c, \eta_a, \eta_b, \eta_c$  – components of the rubbing speed of the infinitesimal friction surface of load  $dS$  in the zones  $a, b$ , and  $c$

$$\begin{aligned} \xi_a = \xi_c = v - \dot{x}_o + \dot{\phi}r \sin \beta & & \xi_b = v \cos \alpha - \dot{x}_o + \dot{\phi}r \sin \beta \\ \eta_a = \eta_c = \dot{y}_o + \dot{\phi}r \cos \beta & & \eta_b = -v \sin \alpha + \dot{y}_o + \dot{\phi}r \cos \beta \end{aligned} \quad (4.7)$$

$v_{o(i)}$  – resulting rubbing speed of the infinitesimal friction surface  $dS$  in the zones  $i = a, b, c$

$$v_{o(i)} = \sqrt{\xi_i^2 + \eta_i^2} \quad (4.8)$$

$\beta$  – inclination angle of radius  $r$

$$\beta = \arctan \frac{y_s - y_o}{x_s - x_o} \quad (4.9)$$

$x_o, y_o, \phi$  – coordinates of the gravity centre  $C_s$  and rotation angle of the load, respectively

$x_s, y_s$  – coordinates of the infinitesimal surface  $dS$

$m_p, I_p$  – mass and mass moment of inertia of the load, respectively

$\mu_i$  – coefficient of friction between the load and conveyor in the zone  $i$ .

## 5. Numerical experiments

In the performed numerical analyses, we assumed the characteristic of the friction coefficient described with a single parameter – according to Fig. 3b. The analysis of discrepancies resulting from the application of the classic, single-parameter characteristic of the friction coefficient in the sorting process model with respect to that applying a curvilinear characteristic modelled with the cubic b-spline curve (Fig. 3f), is presented in Section 6.

Figure 7 depicts the trajectory of motion of the load gravity centre determined as the load scraped by the system of disks set at the angle of  $\alpha = 90^\circ$ . One neglects here the influence of the zone  $c$  on the course of the sorting process assuming an infinitesimally great width of the zone  $b$ . Such an approach allows us to determine the distance at which the manipulated object forces its way into the working space of the manipulator without considering the disturbances resulting from the influence of the zone  $c$  on the work of the manipulator. This influence will be considered in a further part of this study.

In Fig. 7, the continuous line (reference 1) denotes the trajectory of load motion obtained by simulation of the sorting process carried out with the use

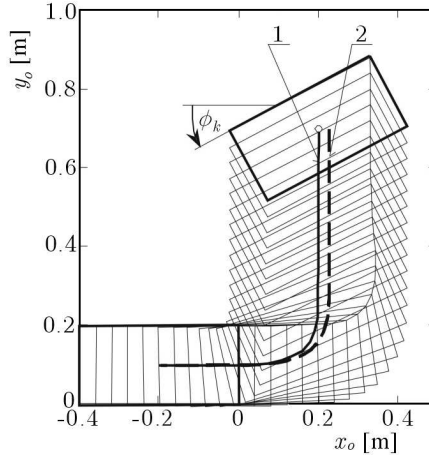


Fig. 7. Trajectory of the load gravity centre during sorting by the manipulator with frictional disks; 1 – moment of friction forces taken into account, 2 – moment of friction forces neglected;  $A \times B = 0.4 \times 0.2$  m,  $v = 1$  m/s,  $\alpha = 90^\circ$ ,  $b \rightarrow \infty$ ,  $\mu_a = \mu_b = 0.6$

of equations (4.1), while the broken line (reference 2) pertains to the case, when the influence of moment of friction forces is neglected. The presence of the moment of friction forces, which are produced by reactions of the manipulator carrying zones, causes that the load is rotated by the angle  $\phi_k$ , and the distance at which the load forces its way into the manipulator working space is shortened.

Neglecting the moment of friction forces in analysis of the load motion significantly speeds up numerical experiments. The estimates of minimal width of the zone  $b$  (necessary for the sorting process to be carried out correctly), which have been determined based on the simplified model, will be taken to further considerations with some excess in order to increase the probability that the object is scrapped correctly.

The transportation speed assumed during the investigations equals  $v = (0.5-1.5)$  m/s, and the dimensions of the load projection on the conveyor surface are  $A \times B = (0.2-1.2) \times (0.2-0.8)$  m. The assumed conveyor speed is equal to that used in roller conveyors (Sempruch and Piątkowski, 2002). The minimal dimension of the object was assumed due to the necessity of taking into account the dead zones in the carrying space located between the disk axes.

Figure 8 presents the results of simulation investigations on the load sorting process aimed at assessing the hazards resulting from difficulties of satisfying the condition of reliable scrapping of the load onto a proper chute. This condi-

tion could be violated because of inadequate translocation of the load towards the chute, in the direction transverse to the conveyor axis.

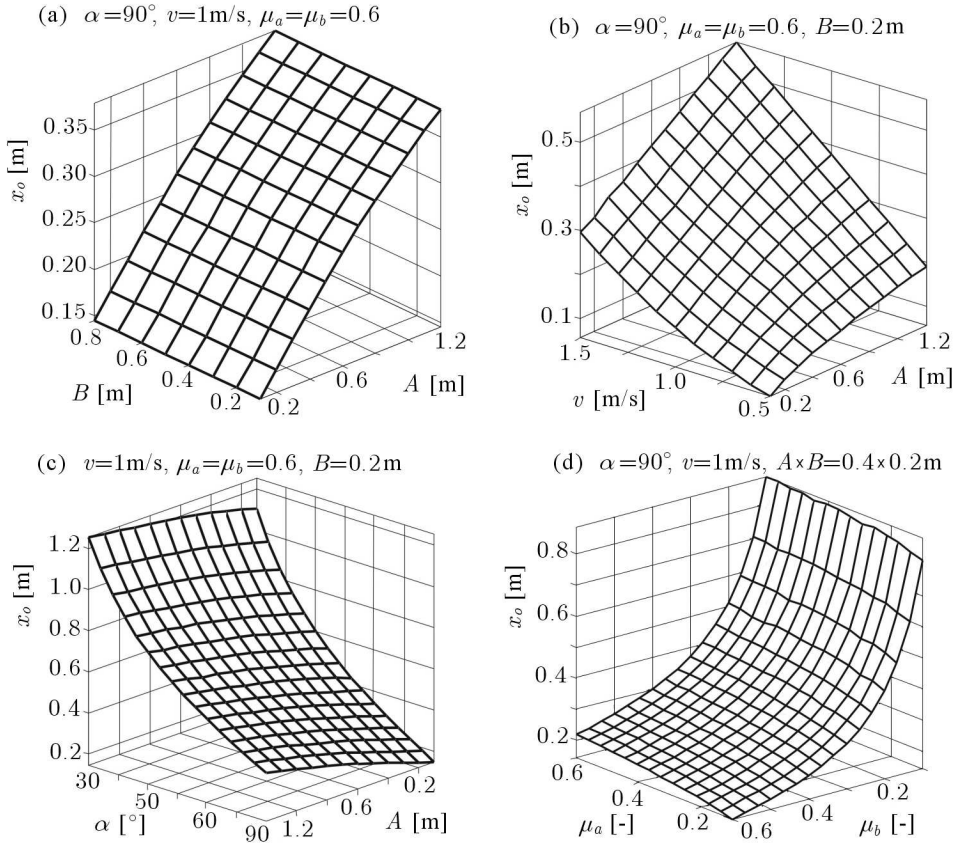


Fig. 8. Distance covered by the gravity centre of the object (during sorting) in the direction of conveyor axis  $x_o$  determined in function of: (a) dimensions of the object  $A \times B$ , (b) transportation speed of the load stream  $v$  and dimension of the load  $A$ , (c) inclination angle of torsional disks  $\alpha$  and dimension of the load  $A$ , (d) friction coefficients  $\mu_a, \mu_b$ ;  $s = 0.7 \text{ m}$  – width of the main conveyor,  $\phi = 0^\circ$ ,  $b \rightarrow \infty$

It was assumed in the analyses that for the load to be scrapped onto a chute its centre of gravity must cover a distance equal to the width of the conveyor  $s = 0.7 \text{ m}$ . The main reason why the load fails to reach the assumed destination place is the insufficient width of the manipulator-load interaction space (zone  $b$ ) relative to the assumed parameters of the sorting process (load dimensions, working angle of the system of disks, transportation speed, frictional properties of the belt conveyor and its operating elements). The necessary

width of the interaction zone is a function of the distance at which the load forces its way in the direction of the axis  $x_o$ . The function is determined without taking into account the influence of the friction zone  $c$ .

From the analysis of Fig. 8a it follows that the distance  $x_o$  depends on the length of the manipulated object (dimension  $A$  – in the case of load position before scraping parallel to the manipulator axis,  $\phi = 0$ ), and is not sensitive to its width  $B$ . The longer the load, the greater the required width of the zone  $b$ .

The load transportation speed  $v$  has the influence on the course of the sorting process similar to that of load dimension  $A$ . The greater the speed value  $v$ , the greater the distance  $x_o$  (Fig. 8b).

The working angle  $\alpha$  of the torsional disk system setting also decides about the required length of the space in which the load is scrapped onto a chute. The influence of this angle on the sorting process is illustrated in Fig. 8c (on the assumption that the new direction of load transportation is reached after the load covers the distance of the conveyor width,  $s = 0.7$  m). The lower the disk setting angle  $\alpha$ , the greater the required width of the zone  $b$  that realises transfer of the load onto a chute.

The relationship between the load friction coefficients in the contact zones  $a$  and  $b$  and the achievable distance  $x_o$  is illustrated in Fig. 8d. From the analysis of Fig. 8d, it follows that the friction coefficient  $\mu_b$  (in the zone  $b$ ) has greater influence on the course of the sorting process than that of the coefficient  $\mu_a$  (in the zone  $a$ ). The greater the value of friction coefficient  $\mu_b$ , the shorter the distance  $x_o$  reached by the load. The friction coefficient  $\mu_a$  has an opposite effect – the lower the value of this coefficient, the more effective translocation of the load onto the chute.

The graphs in Fig. 9 illustrate relationships between the transportation speed of the loads, their lengths and capacity of the sorting process. In these analyses, it was assumed that the load takes a position parallel to the axis of the main conveyor ( $\phi = 0$ ), the working angles of the manipulator disks equal  $\alpha = 90^\circ$  (Fig. 9a),  $\alpha = 45^\circ$  (Fig. 9b), or  $\alpha = 30^\circ$  (Fig. 9c), and that the load must cover a distance of  $s = 0.7$  m in order to be scrapped onto the chute. According to what is shown in Fig. 9a, for the transportation speed  $v = 1.5$  m/s and load length equal to  $A = 0.7$  m, one can achieve technical capacity of the sorting process of approximately  $W_t = 3600$  pcs/h.

When the disk setting angle is set to a lower value,  $\alpha = 45^\circ$  (Fig. 9b), the sorting capacity slightly deteriorates (in comparison to that presented in Fig. 9a – especially in the case of longer objects). When the working angle of the disks equals  $\alpha = 30^\circ$  (Fig. 9c), the drop of sorting capacity looks similar:

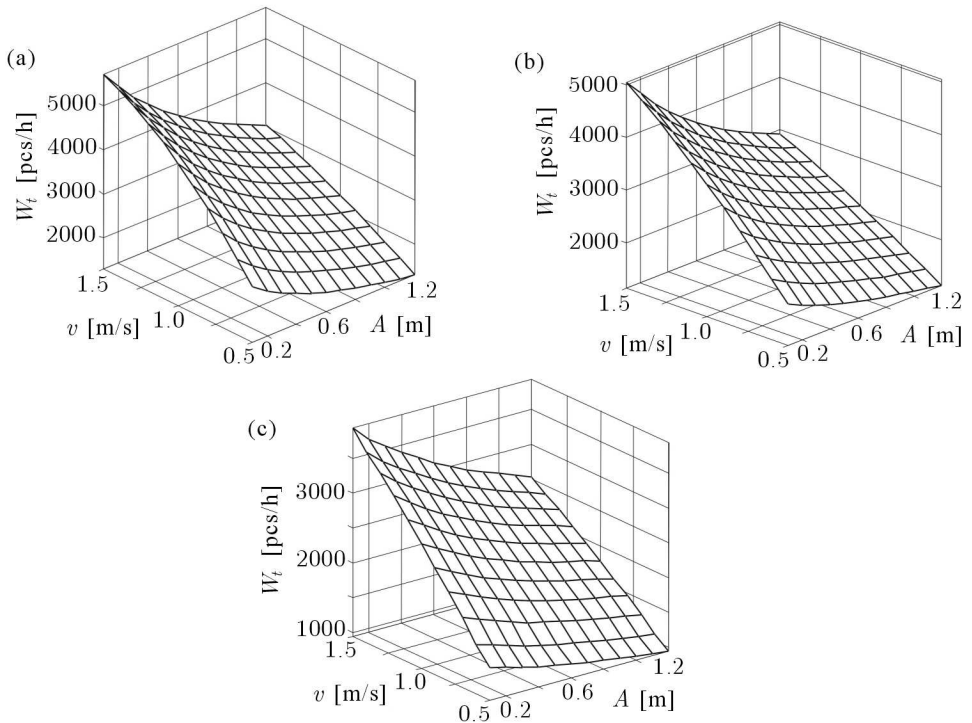


Fig. 9. Influence of the transportation velocity of load stream  $v$  and length of load  $A$  on capacity of the sorting process for: (a)  $\alpha = 90^\circ$ , (b)  $\alpha = 45^\circ$ , (c)  $\alpha = 30^\circ$ ; data:  $\mu_a = \mu_b = 0.6$ ,  $B = 0.2$  m,  $b \rightarrow \infty$

it is more significant in the case of short loads, and less significant for longer loads. The change of the working angle  $\alpha$  does not have any radical effect on the time of scrapping the load onto the chute (especially in the case of long loads), despite the fact that the load scrapped by the system of disks of the working angle  $\alpha = 45^\circ$  (and  $\alpha = 30^\circ$ ) must travel much longer way to the chute than that for the system in which  $\alpha = 90^\circ$ . The obtained effect can be explained by the conditions that exist during the load sorting process – a substantial part of time of load translocation onto the chute is the time of transient motion (stage  $E2$  – Fig. 10). The load scrapped by the system of disks of the working angle  $\alpha = 45^\circ$  (and  $\alpha = 30^\circ$ ) remains for a much shorter period in the state of transient motion (stage  $E2$  – Fig. 10b,c) than that in the case of  $\alpha = 90^\circ$  (Fig. 10a). Additionally, the component of rubbing speed in the direction of the axis  $y_o$  ( $\eta_b$ ), shown in Fig. 10b,c (setting angles of the disk system  $\alpha = 45^\circ$ ,  $\alpha = 30^\circ$ ), is much greater than the component in the direction of the axis  $x_o$  ( $\xi_b$ ). In the same proportion, the component of the friction force in the direction of the axis  $y_o$  ( $F_{\eta_b}$ , Fig. 6) is much greater than

the component of that force in the direction of the axis  $x_o$  ( $F_{\xi_b}$ ), which results in a greater acceleration of the load motion towards the chute. If the working angle of the disk system equals  $\alpha = 90^\circ$ , the components of the load rubbing speed in the directions of the axes  $x_o$  and  $y_o$  are the same ( $\xi_b = \eta_b$ , Fig. 10a), and consequently, the components of the load friction forces (as well as the accelerations) in both directions have the same values.

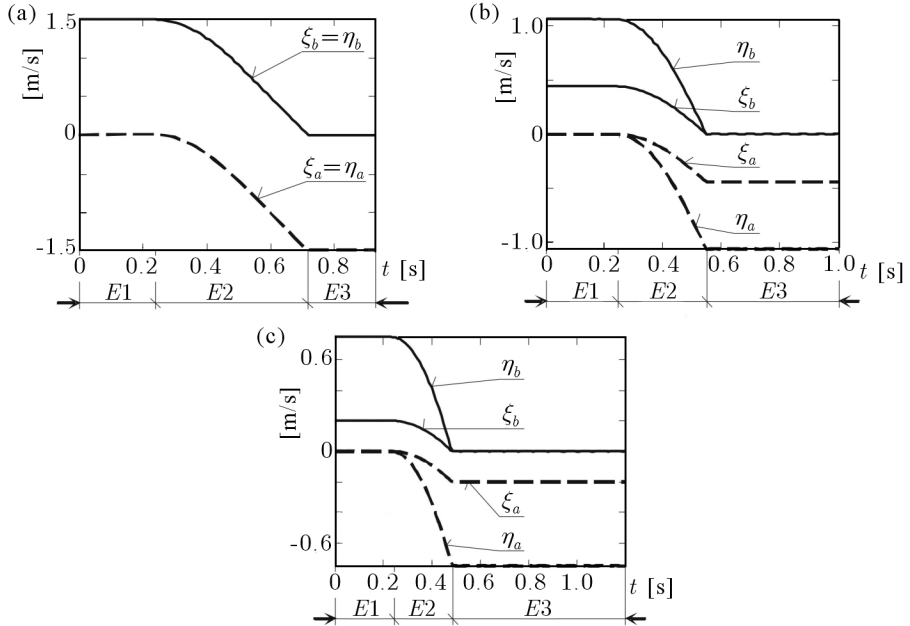


Fig. 10. Graphs of components of the load rubbing speed ( $A \times B = 0.7 \times 0.2$  m) for the working angle of the torsional disk system: (a)  $\alpha = 90^\circ$ , (b)  $\alpha = 45^\circ$ , (c)  $\alpha = 30^\circ$ ; stages of load motion:  $E1$  – steady motion I (sliding in zone  $b$ , no sliding in zone  $a$ ),  $E2$  – transient motion (load sliding in zones  $b$  and  $a$ ),  $E3$  – steady motion II (no load sliding in zone  $b$ );  $v = 1.5$  m/s

In the determination of the required size of the manipulator-object interaction space, one aims at assuming possibly small width of the zone  $b$ , which follows from the condition of minimizing construction costs of the load sorting system. Selecting smaller and smaller widths of the zone  $b$  (and, at the same time, widening the influence of the zone  $c$ ) can be continued, however, up to the moment when (during translocation of the loads onto the chute) the manipulator is able to effectively cause that rubbing of the load against the system of disks disappears (i.e. to obtain  $v_{ab} = 0$ ).

The graph of minimal width of the zone  $b$  versus transportation velocity of the conveyor  $v$  and length of the load  $A$  is presented in Fig. 11 (determi-

ned based on numerical optimization). The analysis of this graph shows that application of the disk setting angle  $\alpha = 90^\circ$  (Fig. 11a) leads to the expected shortening of the required width of the manipulator working space  $b$  – as compared to manipulators in which  $\alpha = 45^\circ$  (Fig. 11b) and  $\alpha = 30^\circ$  (Fig. 11c).

A particularly high difference in the selected zone width (showing the disadvantage of angles  $\alpha = 45^\circ$  and  $\alpha = 30^\circ$ ) appears in the case of low transportation velocity of the conveyor  $v$  and loads of small length  $A$ .

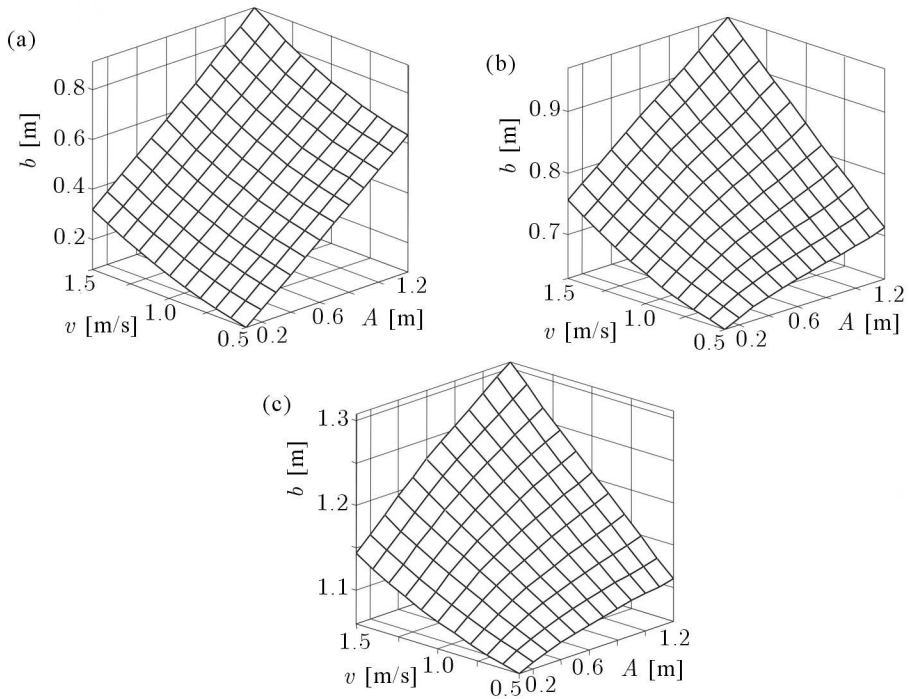


Fig. 11. Minimal width of the manipulator working space  $b$  versus transportation velocity  $v$  and load length  $A$  for: (a)  $\alpha = 90^\circ$ , (b)  $\alpha = 45^\circ$ , (c)  $\alpha = 30^\circ$ ; data:  $\phi = 0^\circ$ ,  $\mu_a = \mu_b = \mu_c = 0.6$

## 6. Evaluation of the influence of friction coefficient characteristics on the course of unit-load manipulation process

The appropriateness of utilizing the classical constant-function characteristics of load coefficients (shown in Fig. 3a,b) in the model of the sorting process is decided on the basis of analysis of numerical investigation results in which

we take into account the characteristics of Fig. 3a,b, and the "reference" one, of Fig. 3f. In these analyses, we assume that the friction coefficient functions shown in Fig. 3f, Fig. 3a and Fig. 3b will be identified as: model 1, model 2 and model 3, respectively. The parameters  $\mu_0$  and  $\mu_G$  that appear in these functions have the values of 0.65 and 0.46, respectively.

The temptation for using the classic friction coefficients follows from the simplicity of mathematical expressions. Frictional properties of bodies represented by the model of Fig. 3a need only two parameters to be determined, and those of Fig. 3b – just one parameter. The characteristic of friction coefficient shown in Fig. 3f requires as much as 12 parameters be determined – 6 control points on the b-spline curve.

The characteristic of Fig. 3f was determined on the basis of experimental investigation results, which consisted in positioning the object by means of a system of two, inversely-driven belts of the conveyor (Fig. 12 – Piątkowski and Sempruch (2006b)). In these investigations, the object was set in damped oscillatory motion (with respect to the equilibrium position that occurs at the boundary of influences of the two frictional sections of the conveyor – Fig. 13a). The simulation of this process with the use of classical friction coefficient models always leads to the same effect – to non-damped oscillatory motion, Fig. 13b. This result proves imperfection of models 2 and 3 in their application. The discrepancy between the results obtained in such a way leads to radically different conclusions. The lack of damping in the oscillatory motion would indicate uselessness of such a method of object positioning and failure of the whole idea.

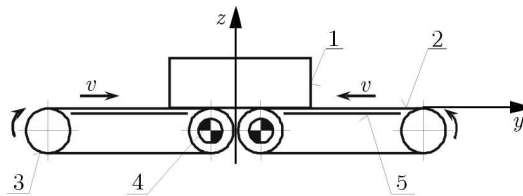


Fig. 12. Scheme of the stand for object positioning: 1 – unit load under test, 2 – conveyor belt, 3 – tension roll, 4 – powered roll, 5 – bed;  $v$  – linear velocity of belt

The courses of friction forces appearing between the object and the carrying surface of the sorting manipulator with torsional disks are shown in Fig. 14. One took the following assumptions:  $\alpha = 45^\circ$ ,  $v = 1.5$  m/s,  $m_p = 5$  kg,  $A \times B = 0.4 \times 0.26$  m,  $s = 0.7$  m,  $b \rightarrow \infty$  (denotations as in Fig. 1 and Fig. 6). The results represented in Fig. 14a pertain to the simulation that utilizes model 1, and those in Fig. 14b – to that based on models 2 and 3. The basic

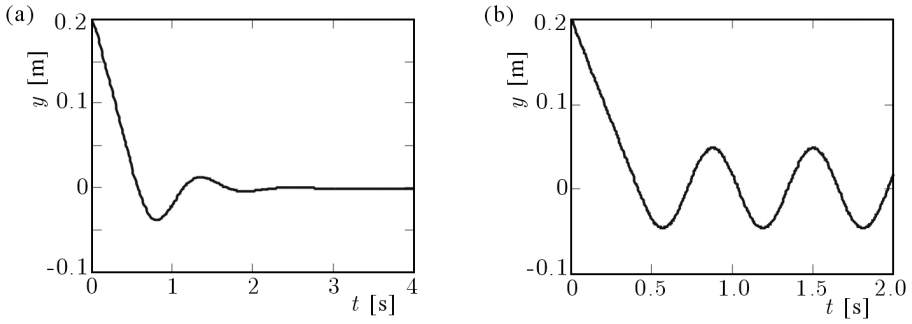


Fig. 13. Trajectory of motion of the load positioned by a system of two inverse fields of friction forces: (a) according to model 1, (b) according to models 2 and 3;  $v = 0.37 \text{ m/s}$ ,  $A \times B = 0.4 \times 0.3 \text{ m}$

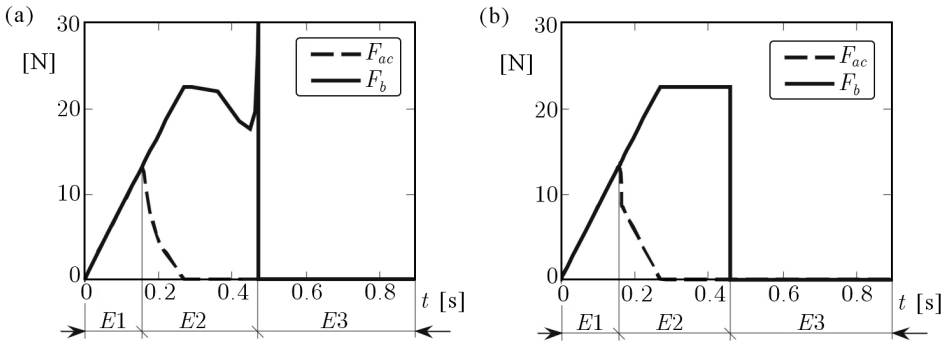


Fig. 14. Friction force  $F$  exerted on the object during sorting by the manipulator with torsional disks: (a) for model 1, (b) for models 2 and 3; stages of load motion, according to Fig. 10:  $E1$  – steady motion I,  $E2$  – transient motion,  $E3$  – steady motion II; remaining data:  $\alpha = 45^\circ$ ,  $v = 1.5 \text{ m/s}$ ,  $m_p = 5 \text{ kg}$ ,  $A \times B = 0.4 \times 0.26 \text{ m}$ ,  $s = 0.7 \text{ m}$ ,  $b \rightarrow \infty$

difference between the presented graphs concerns the course of the friction force  $F_b$  just before the end of its activity. In the case of model 1 (Fig. 14a), in the final interval of stage  $E_2$  (denotation as in Fig. 10) one observes a rapid increase of this force. The influence of the observed difference on the basic sorting process parameters (time of load-scraping cycle  $t_c$  and the required length of the manipulator working space  $L$ ) is illustrated in Fig. 15. The discrepancies between the sorting process parameters determined based on models 1, 2 and 3 are insignificant. The data shown in Fig. 16 (derived based on Fig. 15) justify this conclusion. These data represent relative working parameters of the manipulator, i.e. the results calculated on the basis of models 2 and 3 referred to those obtained by using model 1. The relative discrepancy between

the results based on classic models 2 and 3 and those obtained with model 1 does not exceed 1%.

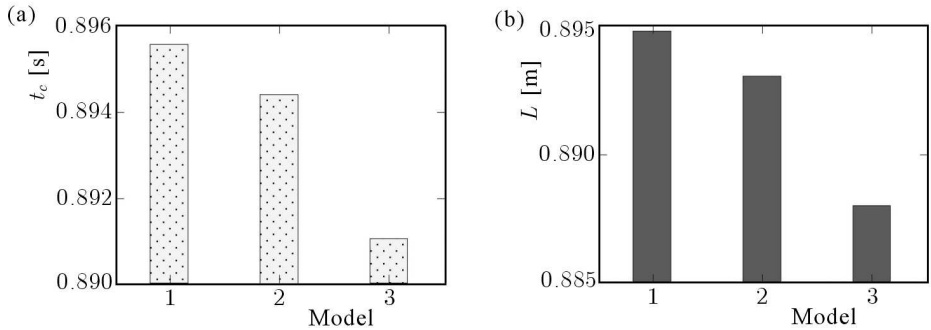


Fig. 15. Working parameters of the manipulator with torsional disks: (a) time of load-scraping cycle, (b) length of the manipulator working space

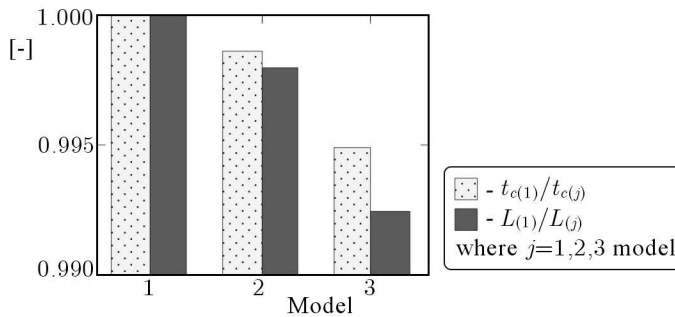


Fig. 16. Relative working parameters of the manipulator with torsional disks,  $t_{c(1)}/t_{c(j)}$  and  $L(1)/L(j)$ , derived based on Fig. 15 (where  $j = 1, 2, 3$ )

It follows from the performed investigations that the nonlinear model of the friction coefficient, proposed by Piątkowski and Sempruch (2006b), has meaning when one needs to represent motion of objects in the case of rubbing speeds close to zero, which remain in this range during a substantial part of realisation of the manipulation process. An example of the process in which such conditions exist is the positioning of loads by means of inverse fields of friction forces. In this process, motion of the load relative to the manipulator carrying surface is made cyclically and frequently at low rubbing speeds. The classic, constant-function friction coefficients are then completely ineffective in this application.

A different situation exists in the case when we deal with the description of the sorting process. This process usually involves high rubbing speeds of lo-

ads and the number of transitions between the states of static and kinematic friction is minimal. The result is that the discrepancies between the simulation results, appearing due to application of different friction coefficient models – type 1, 2 and 3, are insignificant. For this reason, the friction coefficient described by the one-parameter model (Fig. 3b) can be considered as an effective tool for representing the course of the load sorting process.

## 7. Conclusion

The results of investigations on the sorting process model, presented in this work, have a theoretical and practical value as they give a possibility of influencing the design and exploitation of load-distributing systems with frictional disks.

- The classic one-parameter function describing the friction coefficient, applied in this model, realistically represents the nature of the load sorting process. Capacity of this description can be attributed to high rubbing speeds at which the object moves with respect to the manipulator working elements, and to the low number of transitions between the states of static and kinematic friction.
- An increase in the working angle of the disk system in the range of  $\alpha \in (30^\circ, 90^\circ)$  causes that:
  - the required width  $b$  of the manipulator working zone becomes shorter,
  - capacity of the sorting process increases; this increase is more pronounced in the case of short loads and less significant for longer loads,
  - acceleration of motion of the manipulated object towards the chute decreases, and the period of transient motion of the object in this direction becomes longer.
- For the sake of capacity of the sorting process, one should assume possibly high values of the friction coefficient for the disk system, and possibly low values for the carrying surface of the main conveyor; the course of the sorting process is definitely more sensitive to changes of frictional properties of the disk system than to those of the carrying surface of the main conveyor.

- A decrease in length of the manipulator working space (friction zone  $b$ ) can be obtained by dividing the sorting process into two stages: the preliminary and the final one. The manipulator, which realises preliminary sorting, should be installed at the beginning of the unit load stream – before the manipulators that carry out the process of final sorting. The preliminary sorting will allow for shifting the load closer to one of the conveyor borders, according to the predicted direction in which the load will be carried away to a new transportation line.

#### *Acknowledgement*

This work has been financed from the funds for science as a Research Project in the years 2008-2010.

### References

1. AKELLA S., HUANG W.H., LYNCH K.M., MASON M.T., 2000, Parts feeding on a conveyor with a one joint robot, *Algorithmica*, Springer-Verlag, **26**, 313-344
2. AWREJCEWICZ J., 1984, Coefficients identification of dynamic nonlinear dry friction dependence on velocity, *Science Books, Mechanics*, Lodz University Press, **429**, 67, 5-12
3. AWREJCEWICZ J., OLEJNIK P., 2002, Numerical analysis of self-excited by friction chaotic oscillations in two-degrees-of-freedom system using exact Henon method, *Machine Dynamics Problems*, **26**, 4, 9-20
4. BÖHRINGER K.F., DONALD B.R., KAVRAKI L.E., 2000, Part orientation with one or two stable equilibria using programmable force fields, *IEEE Transactions on robotics and automation*, **16**, 2, 157-170
5. HENSEN H.A., 2002, *Controlled Mechanical Systems with Friction*, Ph.D. Thesis, Eindhoven University of Technology
6. KIKUUWE R., TAKESUE N., SANO A., MOCHIYAMA H., FUJIMOTO H., 2005, Fixed-step friction simulation: from classical Coulomb model to modern continuous models, *International Conference on Intelligent Robots and Systems*, 3910-3917
7. KORENDO Z., UHL T., 1998, Modelling and simulation of friction in deriving system of industrial robots, *XVI Ogólnopolska Konferencja Naukowo-Dydaktyczna TMM*, Rzeszów-Jawor, 256-273 [in Polish]
8. KRIVOPLAS A., 1980, *Paketo-formiruyushchie mashiny*, Maszinstrojenije, Moskwa

9. LAOWATTANA D., SATADAECHAKUL W., 1999, Directive motion of a multiple-constrained holonomic system, *First Asian Symposium on Industrial Automation and Robotics*, Thailand, 133-139
10. LUNTZ J.E., MESSNER W., 1997, A distributed control system for flexible materials handling, *IEEE Const. Syst.*, **17**, 22-28
11. LUNTZ J.E., MESSNER W., CHOSSET H., 1997, Parcel manipulation and dynamics with a distributed actuator array: the virtual vehicle, *IEEE International Conference on Robotics and Automation*, **2**, 1541-1546
12. MASON M.T., 1999, Progress in nonprehensile manipulation, *The International Journal of Robotics Research*, **18**, 1129-1141
13. PIĄTKOWSKI T., 2004, Bases of manipulators classification for needs of sorting and positioning unit loads, *Zeszyty Naukowe Wydziału Mechanicznego*, **35**, Wydawnictwo Uczelniane Politechniki Koszalińskiej, 185-192 [in Polish]
14. PIĄTKOWSKI T., SEMPRUCH J., 2006a, Active fence with flexible element in a drive system, *The Archive of Mechanical Engineering*, **53**, 335-354
15. PIĄTKOWSKI T., SEMPRUCH J., 2006b, Experimental tests of dry friction in handling process of unit loads, *Developments in Machinery Design and Control*, **5**, Wydawnictwo Uczelniane ATR w Bydgoszczy, 57-62
16. PIĄTKOWSKI T., SEMPRUCH J., 2008a, Model of inelastic impact of unit loads, *Packaging Technology and Science*, John Wiley & Sons, doi: 10.1002/pts.825
17. PIĄTKOWSKI T., SEMPRUCH J., 2008b, Model of the process of load unit stream sorting by means of flexible active fence, *Mechanism and Machine Theory*, Elsevier, doi:10.1016/j.mechmachtheory.2007.05.004, **43**, 5, 549-564
18. SEMPRUCH J., PIĄTKOWSKI T., 2002, *Technical Facilities of Works Transport*, Wydawnictwo Uczelniane ATR w Bydgoszczy [in Polish]
19. TARNOWSKI W., BARTKIEWICZ S., 1998, *Modelowanie matematyczne i symulacja komputerowa dynamicznych procesów ciągłych*, Wydawnictwo Uczelniane Politechniki Koszalińskiej

### Model i analiza procesu sterowania strumienia ładunków jednostkowych manipulatorem z krążkami skrętnymi

#### Streszczenie

W artykule przedstawiono propozycję modelowania przebiegu procesu sortowania strumienia ładunków jednostkowych realizowanego za pomocą manipulatora z krążkami skrętnymi. W opracowanym modelu uwzględniono, iż na ruch ładunku w przestrzeni pracy manipulatora mają wpływ trzy strefy tarcia: pierwsza strefa obejmująca

oddziaływanie aktywnej powierzchni nośnej manipulatora oraz dwie strefy znajdujące się na przenośniku taśmowym tuż przed i za manipulatorem. Właściwości cierne obiektu reprezentowane są nieliniowym współczynnikiem tarcia wykorzystując krzywą *cubic b-spline*. Na podstawie przeprowadzonych eksperymentów numerycznych modelu sortowania określono wpływ podstawowych parametrów konstrukcyjnych i eksploatacyjnych manipulatora na precyzję i niezawodność przebiegu procesu sortowania potoku ładunków jednostkowych. Uzyskane dane mogą być wykorzystane jako wytyczne podczas projektowania nowych rozwiązań manipulatorów sortujących oraz jako wskazania niezbędne do optymalnej eksploatacji urządzeń już istniejących.

*Manuscript received January 16, 2009; accepted for print May 11, 2009*